# *Microcracks Interaction in Haversian Cortical Bone*

A. Raeisi Najafi[1]; A. R. Arshi[1]; M. R. Eslami[2]; S. Fariborz[2]; M. Moeinzadeh[3]

*ABSTRACT*

Microcracks development in cortical bone occurs when the tissue is subjected to cyclic and fatigue loading. This phenomenon reduces the fracture resistance of bone. The underlying mechanisms governing bone fracture, however, require a more thorough study. To this effect a two-dimensional micromechanical fiber – ceramic matrix composite material model for the tissue is presented in this paper. Here, the interstitial tissue was modeled as a matrix and the osteon was modeled as a fiber, followed by the implementation of the linear elastic fracture mechanics theory. The solution for the edge dislocations, as a Green's functions, was adopted to formulate a system of singular integral equations for the radial microcracks in the matrix in vicinity of the osteon. The effects of microstructural morphology and heterogeneity of haversian cortical bone upon the fracture behavior was investigated by computing the stress intensity factor near the microcracks tips. The results indicated that interaction between osteon and microcracks was limited to the vicinity of the osteon. Furthermore, analysis of the microcrack interactions was an indication of the effects of microcrack configuration upon Stress Intensity Factor in shape of either stress amplification or stress shielding.

*KEYWORDS*

Linear Elastic Fracture Mechanics, Microcrack Interaction, Haversian Cortical Bone, Microstructure, Edge dislocation

## 1. INTRODUCTION

Microcracks are formed in bone due to fatigue and cyclic loading [1-3]. They are associated with a loss of stiffness [4, 5]. It has generally been presumed that the microcracks cause weakness in the bone [5-7]. The accumulation of microcracks in bone could also lead to bone stress (fatigue) fracture and is implicated in the increased susceptibility of older bone to fracture [8, 9]. However, the significance of these microcracks is unknown and the mechanical parameters that govern microcrack behavior have not been characterized [10-13].

Bone is a biological fiber – ceramic matrix composite material [14-16] with varying microstructural arrangements at different scales that provides sites for microcracking [8]. In this composite material, osteons are considered as fibers and interstitial tissue as a matrix. The interface between the osteons and interstitial tissue is also presented by cement line.

Fracture phenomena in the haversian cortical bone are primarily affected by the morphology and heterogeneity of the microstructure [11, 12, 17, 18]. Any variations in these parameters caused by the aging process, on the other hand, make the problem rather more complicated [11, 19, 20]. As an example, the aging process increases the differences in the mechanical properties of osteons and interstitial tissue [19]. This has a profound effect upon the fracture behavior of bone [11, 12]. It was thus necessary to enhance the understanding of the mechanisms governing fracture in haversian cortical bone [18].

Here, the Linear Elastic Fracture Mechanics (LEFM) theory was adopted for the analysis of fracture in composite fiber – ceramic matrix materials [21]. This theory has also been used in determination of the bone resistance to fracture [22-24]. However, only a limited number of efforts have considered fracture micromechanics in the haversian cortical bone [12, 25-27]. Amongst such efforts, Lakes et al (1990) have reported that fracture mechanics of microcracks with lengths of 250-500$\mu m$ in the haversian cortical bone can be predicted by LEFM [25]. Furthermore, Advani et al (1987) have studied the microcrack growth arrest by cement line [27]. In a more recent study, Guo et al (1998) have reported on the osteonal effect on a microcrack which was oriented perpendicularly to the external load [12]. However, a detailed description of the relationship between microcracks and the fracture behavior has not as yet been provided. To understand this relation, it is necessary to begin by formulating a sufficiently encompassing description of microcrack governing micromechanics, accompanied by the description of the interaction of existing microcracks on one another.

The purpose of this study was to investigate the effect of microstructural heterogeneity and morphology on the fracture behavior through adaptation of a simple analytical model. Furthermore, the interaction amongst

[1] Faculty of Biomedical Engineering, Amirkabir University of Technology, Tehran, Iran
[2] Department of Mechanical Engineering, Amirkabir University of Technology, Tehran, Iran
[3] Department of General Engineering, University of Illinois at Urbana - Champaign

microcracks and the fracture governing parameter were also considered.

## 2. METHODS

The assumption of plain strain conditions and linear elastic fracture mechanics in a two-dimensional model of the bone could be justified by the similarities between haversian cortical bone and the composite fiber – ceramic matrix materials. The osteons were represented as fibers and the interstitial tissue was considered as a matrix in this model. The cement line was not included in this model. All the tissues were assumed homogenous. Furthermore, the osteonal interaction was ignored by considering a single osteon. Exclusion of the haversian channel structure, on the other hand, leads to the single osteon being represented by a solid cylinder.

The model consists of a single osteon with the radius $R_0$, and constants of $K_2$ and $G_2$ situated within a matrix resembling the interstitial tissue with constants $K_1$ and $G_1$, as shown in Fig. 1, where $G_i$ is the Shear Modulus and $K_i$, is the Boltzman constant. Boltzman constant is computed as $K_i=3-4\nu_i$ with respect to Poisson's ratio ($\nu$) in plain strain condition. Here, ($n$) radial microcracks, each having a length $2L_i$, were situated within the interstitial tissue. A uniform tensile load of $\sigma_0$ was applied to the model at the infinity. The interface between the osteon and the interstitial tissue was also assumed to be a perfect bonding.

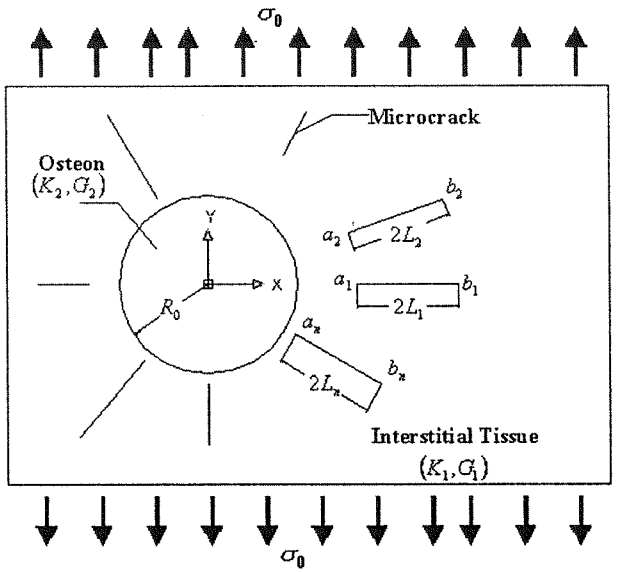


Figure 1: Osteon-interstitial tissue model

It was thus possible to solve the problem as a superposition of two distinct problems. In the first problem, an elastic osteon situated within an infinite elastic plane, similar to interstitial tissue, and without any microcracks was considered. This problem was solved for an external load of $\sigma_0$.

The second problem described stress disturbance due to microcracks in the interstitial tissue. Here, the external loads were limited to the microcrack surface tractions. The external loads were equal in magnitude and opposite in sign to the obtained stress in the presumed location of microcracks as described by the first problem. It should however be noted that formulation of stress equations for individual microcracks does entail the effects of other microcracks. It is apparent that the second problem contains a singularity.

*A. Solutions of Equations of Elasticity, In Polar Coordinates*

Solution of the first problem for a uniaxial tension at infinity is as follow [28]:

$$p_{rr} = \sigma_0[\cos^2\theta - 2G_1(\frac{A}{r^2} + (\frac{2C}{r^2} - \frac{3B}{r^4})\cos 2\theta)] \quad (1a)$$

$$p_{\theta\theta} = \sigma_0[\sin^2\theta + 2G_1(\frac{A}{r^2} - \frac{3B}{r^4}\cos 2\theta)] \quad (1b)$$

$$p_{r\theta} = \sigma_0[-\frac{\sin 2\theta}{2} + 2G_1(\frac{3B}{r^4} - \frac{C}{r^2})\sin 2\theta)] \quad (2c)$$

Where:

$$A = (\frac{R_0^2}{4G_1}) \times (\frac{(K_2-1)-(K_1-1)GR}{2GR+(K_2-1)}) \quad (2a)$$

$$B = (\frac{R_0^4}{4G_1}) \times (\frac{1-GR}{1+K_1GR}) \quad (2b)$$

$$C = (\frac{R_0^2}{2G_1}) \times (\frac{1-GR}{1+K_1GR}) \quad (2c)$$

$$GR = \frac{G_2}{G_1} \quad (2d)$$

Here, $r$ and $\theta$ are polar coordinates where $r$ is measured from the center of the osteon and $\theta$ is measured with respect to the load direction. In providing a solution to the first problem, the shear and normal stress ($p_{ti}$ and $p_{ni}$) at $t$, a point on the location of ith imaginary microcrack, had to be computed.

*B. IntegralEequations*

To solve the second problem, however, dislocation solution [29] could be used. The dislocations Burgers vectors ($b_t$ and $b_n$) were placed along and perpendicular to the microcracks direction, respectively. The shear stress and normal stress values in the microcracks location were equal in magnitude but with opposing signs to those of the first problem [21]. The dislocation density ($B_t$ and $B_n$) at $\xi$, a point on the microcracks, could thus be defined as:

$$\delta b_t = B_t(\xi)d\xi \qquad \xi \in L_i \tag{3a}$$

$$\delta b_n = B_n(\xi)d\xi \qquad \xi \in L_i \tag{3b}$$

Here the microcracks opening displacement and the dislocation density were related by (4) as:

$$u_t(\xi)\Big|_0 - u_t(\xi)\Big|_{2\pi} = -\int_{a_i}^{\xi} B_t(\xi)ds \quad i = 1,2,....,n \tag{4a}$$

$$u_n(\xi)\Big|_0 - u_n(\xi)\Big|_{2\pi} = -\int_{a_i}^{\xi} B_n(\xi)ds \quad a_i \le \xi \le b_i \tag{4b}$$

Since the microcracks opening tips displacement were equal to zero, (6) would have implied:

$$\int_{a_i}^{b_i} B_t(\xi)ds = 0 \tag{5a}$$

$$\int_{a_i}^{b_i} B_n(\xi)ds = 0 \tag{5b}$$

Now, if it is assumed that $b_t$ and $b_n$ are continually distributed over the microcracks, the shear and normal stresses could be formulated as:

$$\sigma_{ti}(t) = \sum_{j=1}^{n} \int_{-1}^{1} \left[k_{t_1}(s,t)b_t(s) + k_{t_2}(s,t)b_n(s)\right] ds \tag{6a}$$

$$\sigma_{ni}(t) = \sum_{j=1}^{n} \int_{-1}^{1} \left[k_{n_1}(s,t)b_t(s) + k_{n_2}(s,t)b_n(s)\right] ds \qquad \text{I, j=1,2,..., n} \tag{6b}$$

The computation method for $k_{t1}$, $k_{t2}$, $k_{n1}$, and $k_{n2}$ are presented in Appendix A. Furthermore, variables $s$ and $t$ in (6) are defined as:

$$x_i = x_{im} + (L_i \cos\alpha_i)t \tag{7a}$$

$$y_i = y_{im} + (L_i \sin\alpha_i)t \tag{7b}$$

$$\xi_i = x_{im} + (L_i \cos\alpha_i)s \tag{7c}$$

$$\eta_i = y_{im} + (L_i \sin\alpha_i)s \tag{7d}$$

In (7), the $x_{im}$ and $y_{im}$ represent the coordinates of the ith microcracks center and $\alpha_i$ is the ith microcracks direction with respect to the horizontal axis.

After separating the singular part from dislocation density, $B_t$ and $B_n$ with respect to the unknown functions $f_t(s)$ and $f_n(s)$ could be defined as:

$$B_t(s) = \frac{f_t(s)}{\sqrt{1-s^2}} \tag{8a}$$

$$B_n(s) = \frac{f_n(s)}{\sqrt{1-s^2}} \tag{8b}$$

Substituting (8) in (5, 6):

$$\sigma_{ti}(t) = \sum_{j=1}^{n} \int_{-1}^{1} [k_{t1}(s,t)\frac{f_t(s)}{\sqrt{1-s^2}} + k_{t2}(s,t)\frac{f_n(s)}{\sqrt{1-s^2}}]ds \tag{9a}$$

$$\sigma_{ni}(t) = \sum_{j=1}^{n} \int_{-1}^{1} [k_{n1}(s,t)\frac{f_t(s)}{\sqrt{1-s^2}} + k_{n2}(s,t)\frac{f_n(s)}{\sqrt{1-s^2}}]ds \qquad \text{i, j=1,2,..., n} \tag{9b}$$

$$\int_{-1}^{1} \frac{f_t(s)}{\sqrt{1-s^2}}\, ds = 0 \tag{10a}$$

$$\int_{-1}^{1} \frac{f_n(s)}{\sqrt{1-s^2}}\, ds = 0 \tag{10b}$$

The unknown functions $f_t(s)$ and $f_n(s)$ could thus be determined by substituting, equal in magnitude and opposite in sign, stress values from the first problem to that of the second:

$$\sigma_{ti}(t) = -p_{ti}(t) \tag{11a}$$

$$\sigma_{ni}(t) = -p_{ni}(t) \tag{11b}$$

*C. Stress Intensity Factors*

The Stress Intensity Factor (*SIF*) in the microcrack tips could be obtained once the functions $f_t(s)$ and $f_n(s)$ were determined:

$$k_I\big|_{s=\pm1} = \pm\frac{2G_1}{k+1}\sqrt{L_i}\, f_n(\pm1) \tag{12a}$$

$$k_{II}\big|_{s=\pm1} = \pm\frac{2G_1}{k+1}\sqrt{L_i}\, f_t(\pm1) \tag{12b}$$

The derivation of expression (12) is provided in Appendix B.

## 3. RESULTS

A radial microcrack, as shown in Fig. 2, with a constant length perpendicular to the external loading was considered in the interstitial tissue. The mode *I* stress intensity factor ($K_I$) variation in the proximal microcrack tip is shown for this condition with respect to the microcrack distance ($d$) to the osteon in Fig. 2. Here, the

reduction of ($d$) was found to be accompanied by an increase in ($K_I$), when the osteon was considered softer than the interstitial tissue ($GR$<1.0). When the osteon was harder than the interstitial tissue ($GR$>1.0), on the other hand, the SIF was found to decrease as ($d$) was reduced. The results have shown the interaction between the osteon and microcracks was limited to vicinity of the osteon.

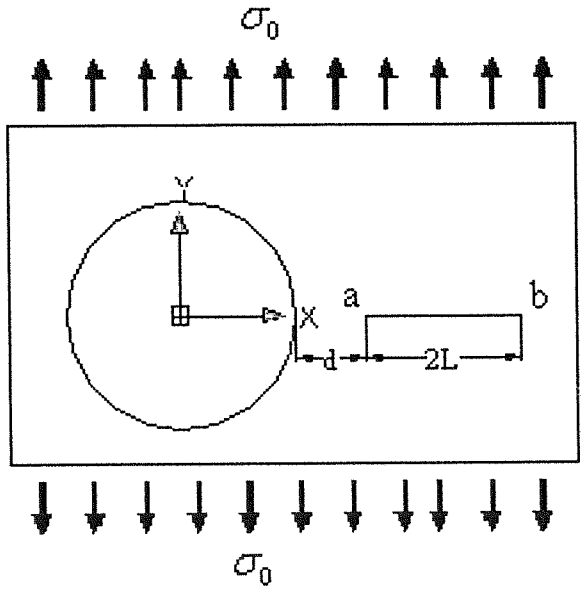


(Figure 2-a)

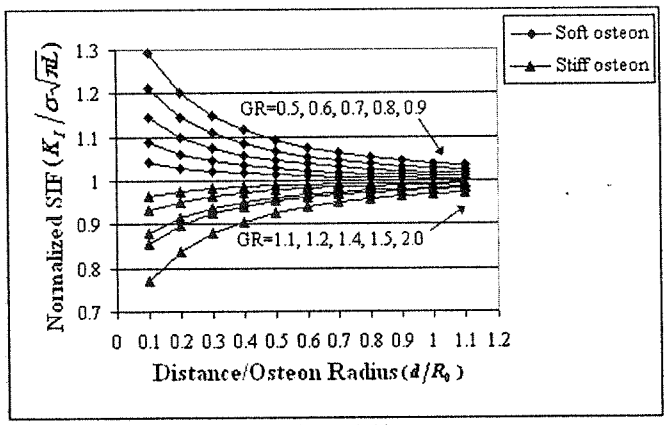


(Figure 2-b)

Figure 2: The normalized SIF of microcrack tips versus the normalized distance ($d/R_0$) from the osteon. Interaction between osteon and the microcrack is limited to the vicinity of the osteon.

To analyze of microcracks interaction upon one another, two microcracks, with a distance ($d$) apart, were considered as indicated by Fig. 3. The existence of another microcrack increases the stress intensity factor ($SIF$) at crack tips as shown in Fig (3). In fact, the figure is showing the stress amplification in SIF. This interaction was significantly reduced as ($d$) was increased. The reduction, however, approached a limit set by the value of $SIF$ for a single microcrack.

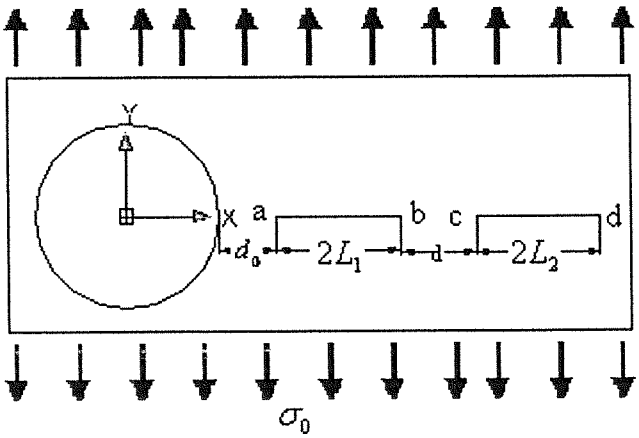


(Figure 3-a)

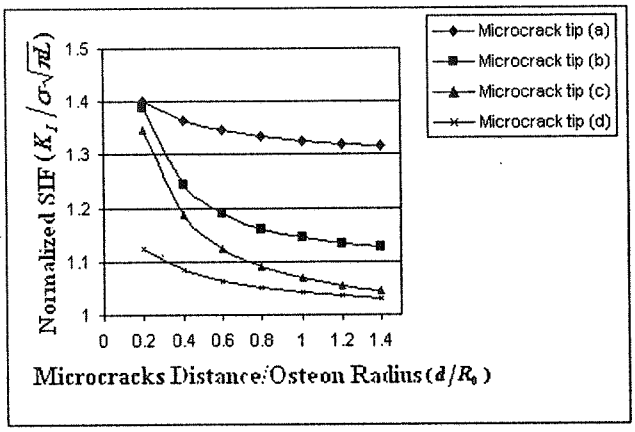


(Figure 3-b)

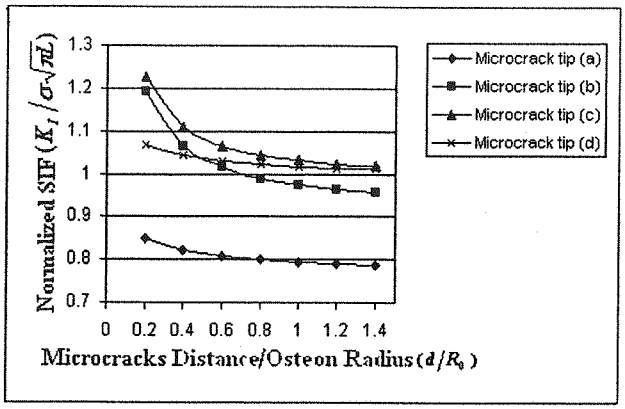


(Figure 3-c)

Figure 3: The normalized SIF of microcrack tips versus the normalized distance between two microcracks ($d/R_0$) when $L_1=L_2$. Figure shows "stress amplification" effect: a) Model, b) Soft osteon ($GR=0.5$), c) Stiff osteon ($GR=2.0$).

In Fig. (4) could be found that microcrack distance from each other and microcrack length could be also affected upon the microcracks interaction. Figure (3-a) shows that as the microcracks distance ($d$) decreased and second microcrack length ($2L_2$) increased, the stress amplification effect was found to increase.

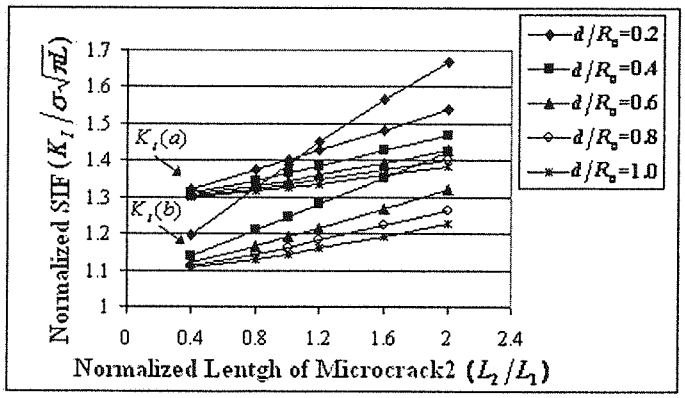


(Figure 4-a)

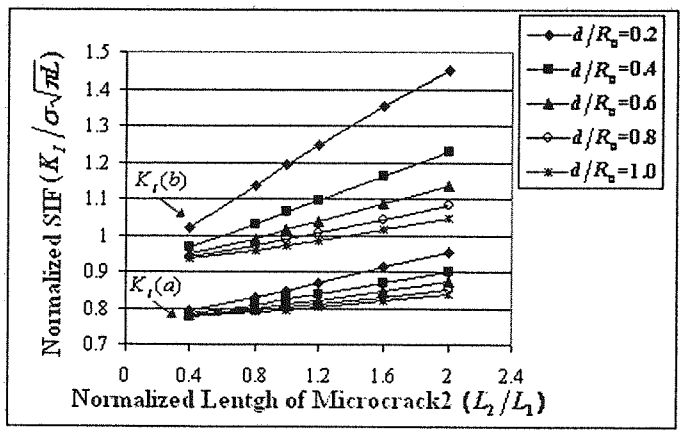


(Figure 4-b)

Figure 4: The normalized *SIF* of microcrack tips versus the normalized length of microcrack 2 ($L_2/L_1$). a) Soft osteon ($GR=0.5$), b) Stiff osteon ($GR=2.0$).

The SIF variation in modes *I* and *II* ($K_I$ and $K_{II}$), when the radial microcrack angle ($\alpha$) changed with respect to horizontal axis, is shown in Fig. 5. The figure indicates that $K_I(a)$ and $K_I(b)$ were reduced as the angle ($\alpha$) was increased. Here, the *SIF* in mode *II* was found to rise as ($\alpha$) was increased to 45 degrees. A reduction of *SIF* was, however, observed as the angle was further increased.

The mutual effect of two microcracks upon one another, when there was an angle ($\alpha$) between them, is shown in Fig. 6. As it can be observed, the first microcrack was assumed to be located along the horizontal axis. The second microcrack was orientated to make an angle ($\alpha$) to the first. In such a situation, the $K_I(a)$ and $K_I(b)$ associated with the first microcrack tips were found to be reduced by the existence of the second microcrack. Of course, *SIF* reduction was affected by the length of secondary microcrack. The interaction of microcracks was an indication of stress shielding. This effect was, however, reduced as the angle ($\alpha$) increased. This reduction approached a limit set by the value of *SIF* for a single microcrack .

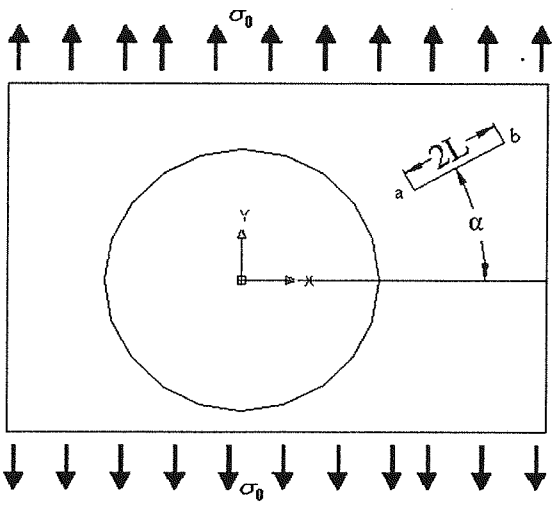


(Figure 5-a)

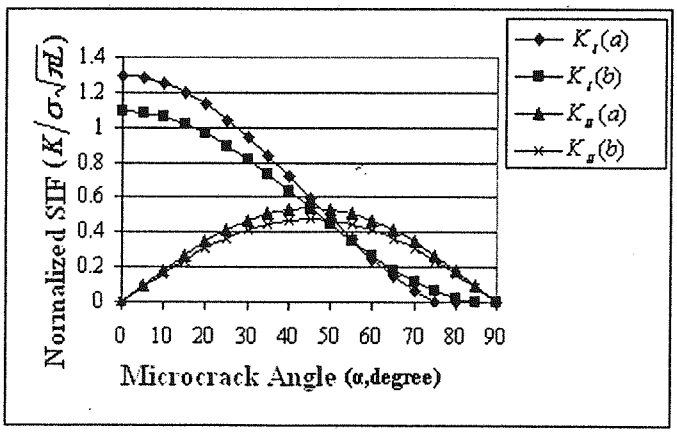


(Figure 5-b)

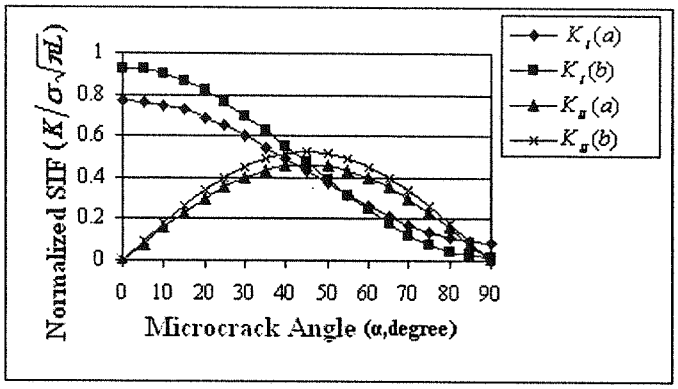


(Figure 5-c)

Figure 5: The normalized *SIF* of microcrack tips versus microcrack angle ($\alpha$). a) Model, b) Soft osteon ($GR=0.5$), c) Stiff osteon ($GR=2.0$).

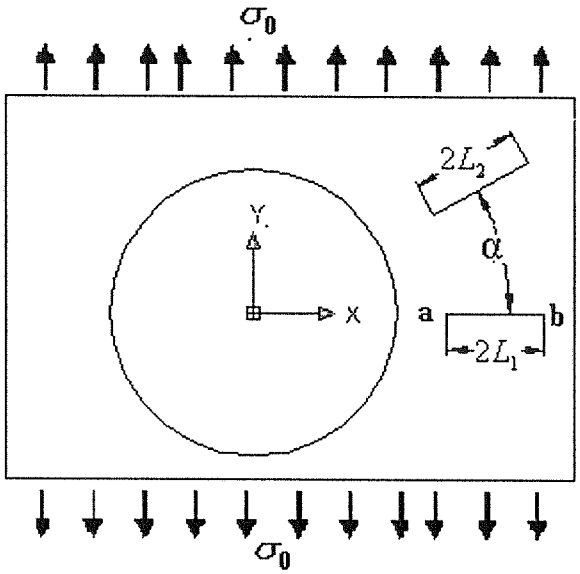


(Figure 6-a)

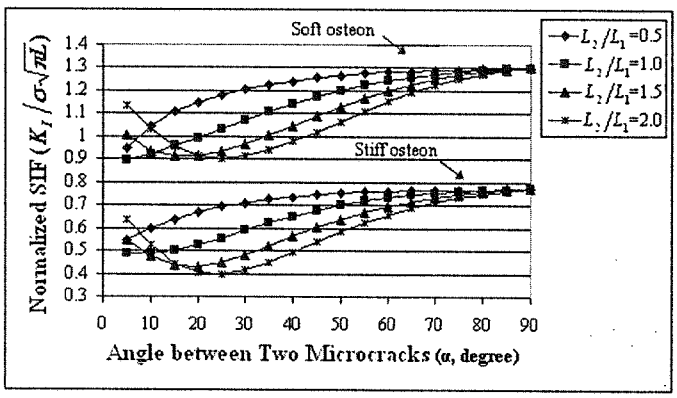


(Figure 6-b)

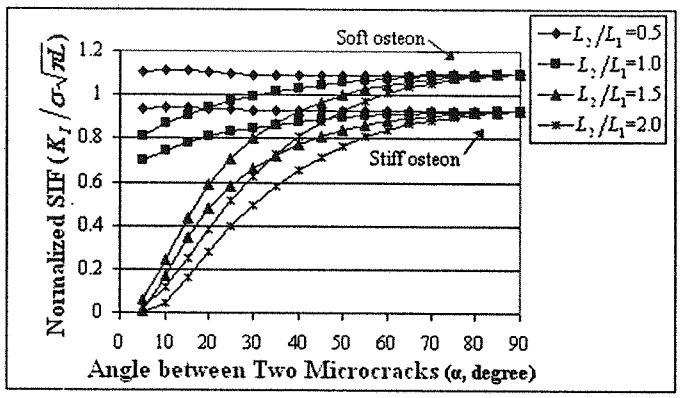


(Figure6-c)

Figure 6: The normalized *SIF* of microcrack tips versus the angle ($\alpha$) between two microcracks. Figure indicates "stress shielding" effect. a) Model, b) *SIF* at tip (a), c) *SIF* at tip (b).

## 4. DISCUSSION

This effort represents a study of fracture micromechanics of haversian cortical bone through adoption of a simplified model. The simplifications were based on a number of fundamental assumptions. One such assumption has been the adoption of LEFM. The application of this theory was based on the results of experimental efforts found in the literature. These results indicate that bone fracture follow linear elastic patterns [22-24]. Furthermore, Robertson et al (1978) have reported that the plastic zone on the microcrack tips was approximately 1-5$\mu m$ which was negligible in comparison to microcrack size [30]. The microcracks were assumed to be situated within the interstitial tissue in this paper. Similar point has also been raised in the results of in – vivo experiments [2, 15]. Two phenomena of cement line debonding and osteon pullout were not included in the current study as the cement line was not considered in the preparation of the model. However, the placement of the microcracks at a distance to the cement line boundary ensures that the exclusion of the cement line does not adversely affect the modeling results. The other simplifying factor was consideration of a single osteon away from others. Consideration of an isolated osteon could not, however, play a decisive factor as the results have shown that the effect of osteon on fracture behavior was limited to the vicinity of the osteon. Another simplification was the exclusion of the haversian channel in the model. The inclusion of the channel would have reduced the effective modulus of the osteon, thereby increasing the effect on the *SIF* at the microcrack tips. The placement of microcracks outside the osteon, however, did reduce the effect of haversian channel exclusion upon microcrack fracture behavior.

The results were a clear indication of the effect of microstructure heterogeneity upon haversian cortical bone fracture behavior. The effect of microstructure heterogeneity upon bone fracture behavior is primarily observed in the

mechanical properties of tissues. It was shown that the osteonal effect upon microcracks changed as the mechanical properties of various microstructural tissues varied. These results were in accordance with other experimental and theoretical reports [11, 12]. Differences in mechanical properties of osteonal and interstitial tissues results in different deformations when the bone is subjected to an applied load. Localized stress concentrations could consequently occur at the interfaces [11]. This stress concentration affects the stress fields at the microcrack tips.

Experimental results indicate that the difference in mechanical properties associated with the osteons and interstitial tissues vary with age, disease, gender and genetic factors [18, 31]. As an example the bone remodeling associated with aging process causes the secondary osteon to contain new bone in comparison to the interstitial region [11]. The mechanical properties of the osteon are expected to remain constant while the remodeling process during aging is sustained [11]. The properties associated with interstitial tissue, however, do not remain constant with aging [11]. This has a severe effect on the bone fracture mechanics. It could be argued that the underlying reason for an increased susceptibility of bone to fracture is due to changes in the mechanical properties of different tissues in the bone.

The results of this paper have shown that the effects of microcracks upon one another could lead to amplification or shielding of the stress intensity factor. This effect was, however, shown to be dependant upon the way microcracks were located with respect to each other. It could therefore be argued that fracture parameters were influenced by the interaction between microcracks. Other experimental results have also point to direct relationship between microcracks and fracture behavior [32] in such a way that reduction of bone resistance to fracture has been found to be accompanied by the coalescence of microcracks [8, 33].

In conclusion, the results of this paper emphasize the effect of microstructure morphology and heterogeneity upon fracture behavior. The accompanying mathematical formulations could also be considered as a further confirmation of the findings of this paper towards analysis of the parameters governing the fracture behavior. Further research towards providing a more detailed model through inclusion of the cement line debonding and osteon pullout and the effect of microcracks on each other's growth trajectories would be valuable.

## 5. APPENDIX

*A: Singular Integral Equations*

The matrix consists of two edge dislocations with Burgers vectors $b_x$ and $b_y$ at the point s ($x_s=\xi$) on x axis (Fig. A1). Stress for any point as $P(x, y)$ on the matrix could be determined as:

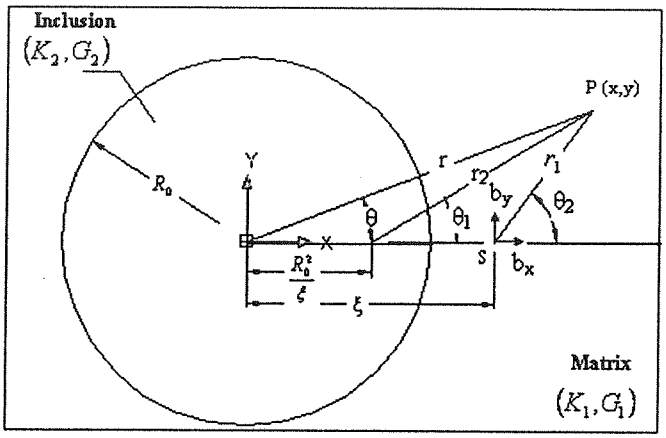


Figure A1: The edge dislocations $b_x$ and $b_y$ in the neighborhood of an inclusion.

$$\sigma_{xx} = k_{xx1}(x,y,\xi)b_x + k_{xx2}(x,y,\xi)b_y \qquad \text{(A1-1)}$$

$$\sigma_{yy} = k_{yy_1}(x,y,\xi)b_x + k_{yy_2}(x,y,\xi)b_y \qquad \text{(A1-2)}$$

$$\sigma_{xy} = k_{xy_1}(x,y,\xi)b_x + k_{xy_2}(x,y,\xi)b_y \qquad \text{(A1-3)}$$

In (A1) the variables are defined as:

$$k_{xx_1}(x,y,\xi) = \frac{G_1}{\pi(k_1+1)R_0}\{-2(1+\frac{2x_1^2}{r_1^2})\frac{y_1 R_0}{r_1^2} + (A + B + 4A\frac{x_2^2}{r_2^2})\frac{R_0 y_2}{r_2^2} - 2A\frac{(\beta^2-1)}{\beta^3}[2x_2 - 8\frac{x_2^3}{r_1^2} - \frac{(\beta^2-1)}{\beta}R_0(1-\frac{4x_2^2}{r_2^2})]\frac{R_0^2 y_2}{r_2^4} - (A+B+4A\frac{x^2}{r^2})\frac{R_0 y}{r^2} - (B-A)\frac{1}{\beta}(\frac{2xyR_0^2}{r^4}) - 2A(1-\frac{4x^2}{r^2})\frac{R_0^3 y}{r^4}\} \qquad \text{(A2-1)}$$

$$k_{xx_2}(x,y,\xi) = \frac{G_1}{\pi(k_1+1)R_0}\{-2(1-\frac{2x_1^2}{r_1^2})\frac{x_1 R_0}{r_1^2} + (A + B - 4A\frac{x_2^2}{r_2^2})\frac{R_0 x_2}{r_2^2} + 2A\frac{(\beta^2-1)}{\beta^3}[\beta^2(-1+\frac{2x_2^2}{r_2^2}) - (6\frac{x_2^2}{r_2^2} - \frac{8x_2^4}{r_2^4}) + \frac{(\beta^2-1)}{\beta}R_0(3-\frac{4x_2^2}{r_2^2})\frac{x_2}{r_2^2}]\frac{R_0^2}{r^2} - (A+B-4A\frac{x^2}{r^2})\frac{R_0 x}{r^2} + [A(2\beta^2-1)+M(k_2+1) - 1]\frac{1}{\beta}(1-\frac{2x^2}{r^2})\frac{R_0^2}{r_2} + 2A(3-4\frac{x^2}{r_2})\frac{R_0^3 x}{r^4}\} \qquad \text{(A2-2)}$$

$$k_{yy_1}(x,y,\xi)=\frac{G_1}{\pi(k_1+1)R_0}\{-2(1-\frac{2x_1^{\,2}}{r_1^{\,2}})\frac{y_1R_0}{r_1^{\,2}}+$$
$$(3A-B-4A\frac{x_2^{\,2}}{r_2^{\,2}})\frac{R_0y_2}{r_2^{\,2}}-2A\frac{(\beta^2-1)}{\beta^3}[-6x_2+\frac{8x_2^{\,3}}{r_2^{\,2}}+$$
$$\frac{(\beta^2-1)}{\beta}R_0(1-4\frac{x_2^{\,2}}{r_2^{\,2}})]\frac{R_0^{\,2}y}{r_2^{\,4}}-(3A-B-4A\frac{x^2}{r^2})\frac{R_0y}{r^2}$$
$$+(B-A)\frac{1}{\beta}(\frac{2xyR_0^{\,2}}{r^4})+2A(1-4\frac{x^2}{r^2})\frac{R_0^{\,3}y}{r^4}\}$$
(A2-3)

$$k_{yy_2}(x,y,\xi)=\frac{G_1}{\pi(k_1+1)R_0}\{2(3-\frac{2x_1^{\,2}}{r_1^{\,2}})\frac{x_1R_0}{r_1^{\,2}}-(5A+B$$
$$-4A\frac{x_2^{\,2}}{r_2^{\,2}})\frac{R_0x_2}{r_2^{\,2}}-A\frac{(\beta^2-1)}{\beta^3}[2(2-\beta^2)-4(5-\beta^2)\frac{x_2^{\,2}}{r_2^{\,2}}+\frac{16x_2^{\,4}}{r_2^{\,4}}$$
$$+2\frac{(\beta^2-1)}{\beta}(3-\frac{4x_2^{\,2}}{r_2^{\,2}})\frac{R_0x_2}{r_2^{\,2}}]\frac{R_0^{\,2}}{r_2^{\,2}}+(5A+B-4A\frac{x^2}{r^2})\frac{R_0x}{r^2}-$$
$$[A(2\beta^2-1)+M(k^2+1)-1]\frac{1}{\beta}(1-\frac{2x^2}{r^2})\frac{R_0^{\,2}}{r^2}-2A(3-4\frac{x^2}{r^2})\frac{R_0^{\,3}x}{r^4}\}$$
(A2-4)

$$k_{xy_1}(x,y,\xi)=\frac{G_1}{\pi(k_1+1)R_0}\{-2(1-\frac{2x_1^{\,2}}{r_1^{\,2}})\frac{R_0x_1}{r_1^{\,2}}+(3A$$
$$-B-4A\frac{x_2^{\,2}}{r_2^{\,2}})\frac{R_0x_2}{r_2^{\,2}}-2A\frac{(\beta^2-1)}{\beta^3}[1-8\frac{x_2^{\,2}}{r_2^{\,2}}+8\frac{x_2^{\,4}}{r_2^{\,4}}+$$
$$\frac{\beta^2-1}{\beta}(3-4\frac{x_2^{\,2}}{r_2^{\,2}})\frac{R_0x_2}{r_2^{\,2}}]\frac{R_0^2}{r_2^{\,2}}-(3A-B-4A\frac{x^2}{r^2})\frac{R_0x}{r^2}$$
$$-(B-A)\frac{1}{\beta}(1-2\frac{x^2}{r^2})\frac{R_0^{\,2}}{r^2}+2A(3-4\frac{x^2}{r^2})\frac{R_0^{\,3}x}{r^4}\}$$
(A2-5)

$$k_{xy_2}(x,y,\xi)=\frac{G_1}{\pi(k_1+1)R_0}\{-2(1-\frac{2x_1^{\,2}}{r_1^{\,2}})\frac{R_0y_1}{r_1^{\,2}}+(A+B-$$
$$4A\frac{x_2^{\,2}}{r_2^{\,2}})\frac{R_0y_2}{r_2^{\,2}}+2A\frac{(\beta^2-1)}{\beta^3}[2\beta^2x_2-4(x_2-2\frac{x_2^{\,3}}{r_2^{\,2}})+$$
$$\frac{\beta^2-1}{\beta}R_0(1-4\frac{x_2^{\,2}}{r_2^{\,2}})]\frac{R_0^{\,2}y_2}{r_2^{\,4}}-(A+B-4A\frac{x^2}{r^2})\frac{R_0y}{r^2}-$$
$$[A(2\beta^2-1)+M(k_2+1)-1]\frac{2}{\beta}\frac{R_0^2xy}{r^4}+2A(1-4\frac{x^2}{r^2})\frac{R_0^3y}{r^4}\}$$
(A2-6)

$$x_1=x-\xi,r_1^{\,2}=x_1^{\,2}+y^2 \quad \text{(A3-1)}$$

$$x_2=x-\frac{R_0^{\,2}}{\xi},r_2^{\,2}=x_2^{\,2}+y^2 \quad \text{(A3-2)}$$

$$r^2=x^2+y^2,\beta=\frac{\xi}{R_0} \quad \text{(A3-3)}$$

$$A=\frac{1-GR}{1+GRk_1} \quad \text{(A4-1)}$$

$$B=\frac{k_2-GRk_1}{k_2+GR} \quad \text{(A4-2)}$$

$$M=\frac{GR(k_1+1)}{(k_2+GR)(k_2-1+2GR)} \quad \text{(A4-3)}$$

The resulting stress obtained through dislocation distribution $b_t$ and $b_n$ in the tangential and normal direction of microcracks could be expressed as:

$$\sigma_{ti}(t)=\sum_{j=1}^{n}\int_{-1}^{1}[k_{t_1}(s,t)b_t(s)+k_{t_2}(s,t)b_n(s)]\,ds \quad \text{(A5-1)}$$

$$\sigma_{ni}(t)=\sum_{j=1}^{n}\int_{-1}^{1}[k_{n_1}(s,t)b_t(s)+k_{n_2}(s,t)b_n(s)]\,ds \quad \text{i, j=1,2,..., n} \quad \text{(A5-2)}$$

Where:

$$k_{t1}=\{k_{xx1}(\frac{-\sin(2\alpha_{ij})}{2})+k_{yy1}(\frac{\sin(2\alpha_{ij})}{2})+k_{xy1}\cos(2\alpha_{ij})\}\times L_j \quad \text{(A6-1)}$$

$$k_{t2}=\{k_{xx2}(\frac{-\sin(2\alpha_{ij})}{2})+k_{yy2}(\frac{\sin(2\alpha_{ij})}{2})+k_{xy2}\cos(2\alpha_{ij})\}\times L_j \quad \text{(A6-2)}$$

$$k_{n1}=\{k_{xx1}\sin^2(\alpha_{ij})+k_{yy1}\cos^2(\alpha_{ij})-k_{xy1}\sin(2\alpha_{ij})\}\times L_j \quad \text{(A6-3)}$$

$$k_{n2}=\{k_{xx2}\sin^2(\alpha_{ij})+k_{yy2}\cos^2(\alpha_{ij})-k_{xy2}\sin(2\alpha_{ij})\}\times L_j \quad \text{(A6-4)}$$

In (A6) $\alpha_{ij}$ could be defined as follow:

$$\alpha_{ij}=\alpha_j-\alpha_i \quad \text{(A7)}$$

*B: Stress Intensity Factor (SIF) Computation* The relationships between crack opening in different fracture modes ($g_t$, $g_n$) and the *SIFs* ($K_I$, $K_{II}$) could be expressed as:

$$\frac{dg_n}{dr}=\frac{k+1}{2G}\frac{k_I}{\sqrt{2\pi r}} \quad \text{(B1-1)}$$

$$\frac{dg_t}{dr}=\frac{k+1}{2G}\frac{k_{II}}{\sqrt{2\pi r}} \quad \text{(B1-2)}$$

The relation between crack opening and dislocation density, on the other hand, could be described as:

$$g_n(r)=\int_0^r B_n(r)dr \quad \text{(B2-1)}$$

$$g_t(r)=\int_0^r B_t(r)dr \quad \text{(B2-2)}$$

The resulting, *SIFs* ($K_I$, $K_{II}$) could thus be obtained by substituting (8) in (B1) and (B2):

$$k_I\big|_{s=\pm1}=\pm\frac{2G_1}{k+1}\sqrt{L_i}\,f_n(\pm1) \quad \text{(B3-1)}$$

$$k_{II}\big|_{s=\pm 1} = \pm \frac{2G_1}{k+1} \sqrt{L_i}\, f_i(\pm 1) \qquad \text{(B3-2)}$$

## 6. REFERENCES


[1] P. Zioupos and J. D. Currey, "The extent of microcracking and the morphology of microcracks in damage bone", J Material Science, vol. 29, pp. 978-986, 1994.

[2] D. B. Burr and T. Stafford "Validity of the bulk-staining technique to separate artifactual from In Vivo microdamage", Clinical Orthopaedics and Related Research, vol. 260, pp. 305-308, 1990.

[3] R. B. Martin, "Mathematical model for repair of fatigue damage and stress fracture in osteonal bone", J Orthopaedic Research, vol. 13, pp. 309-316, 1995.

[4] D. B. Burr, C. H. Turner, P. Naick, M. R. Forwood, W. Ambrosius, M. Sayeed Hasan, R. Pidaparti, "Does microdamage accumulation affect the mechanical properties of bone?" J. Biomechanics, vol. 31, pp. 337-345, 1998.

[5] M. B. Schaffler, K. Choi, and C. Milgrom, "Aging and matrix microdamage accumulation in human compact bone", Bone, vol. 17, pp. 521-525, 1995.

[6] M. R. Forwood and A. W. Parker, "Microdamage in response to repetitive tensional loading in the rat tibia ", Calcified tissue international, vol. 45, pp. 47-53, 1989.

[7] T. L. Norman and Z. Wang "Microdamage of human cortical bone: Incidence and morphology in long bones ", Bone, vol. 20(4), pp.375-379, 1997.

[8] Y. N. Yeni and D. P. Fyhrie "Fatigue damage-fracture mechanics interaction in cortical bone", Bone, vol. 30(3), pp. 509-514, 2002.

[9] S. Sherman, R. P. Heaney, A. M. Parfitt, E. V. Hadley, C. Dutta, " NIA workshop on aging and bone quality", Calcified tissue international, vol. 53, (suppl. 1), 1993.

[10] G. C. Reily and J. D. Currey, "The effects of damage and microcracking on the impact strength of bone" J Biomechanics, vol. 33, pp. 337-343, 2000.

[11] J. B. Phelps, G. B. Hubbard, X. Wang., C. M. Agrawal, "Microsructural heterogeneity and the fracture toughness of bone ", J Biomedical Material Research, vol. 51, pp. 735-741, 2000.

[12] X. R. Guo, L. C. Liang, and S. A. Goldstein, "Micromechanics of osteonal cortical bone fracture ", J Biomechanical Engineering, vol. 120, pp.112-117, 1998.

[13] O. Akkus, D. T. Davy, and C. M. Rimnac, "Microdamage coalescence mechanisms in human cortical bone", 23rd Annals meeting of the American society of biomechanics, University of Pittsburgh, October 21-23, 1999.

[14] H. A. Hogan, "Micromechanics modeling of haversian cortical bone properties" J Biomechanics, vol. 25(5), pp.549-556, 1992.

[15] P. J. Prendergast and R. Huiskes, "Microdamage and osteocyte-lacuna strain in bone: A microstructural finite element analysis " J Biomechanical Engineering, vol. 118, pp. 240-246, 1996.

[16] P. Braidotti, F. P. Branca, E. Sciubba, L. Stagni, "An elastic compound tube model for a single osteon", J Biomechanics, vol. 28(4), pp. 439-444, 1995.

[17] C. Fleck and D. Eifler, "Deformation behavior and damage accumulation of cortical bone specimens from the equine tibia under cyclic loading ", J Biomechanics, vol. 36(2), pp. 179-189, 2003.

[18] M. Doblaré, J. M. García and M. J. Gómez, " Modeling bone tissue fracture and healing: a review ", Engineering Fracture Mechanics, vol. 71(13-14), pp.1809-1840, 2004.

[19] E. D. Simmons, K. P. H. Pitzker, and M. D. Grynpas, "Age-related changes in the human femoral cortex", J Orthopaedic Research, vol. 9, pp. 155-167, 1991.

[20] R.K. Nalla, J.J. Kruzic, J.H. Kinney and R.O. Ritchie, "Effect of aging on the toughness of human cortical bone: evaluation by R-curves", Bone, vol. 35 (6), pp. 1240-1246, 2004.

[21] F. Erdogan, G. D. Gupta, and M. Ratwani, "Interaction between a circular inclusion and an arbitrarily oriented crack", J Applied Mechanics, December, pp. 1007-1013, 1974.

[22] W. Bonfield, "Advances in the fracture of cortical bone", J Biomechanics, vol. 20(11/12), pp. 1071-1081, 1987.

[23] J. M. Melvin, "Fracture mechanics of bone" J Biomechanical Engineering, vol. 115, pp. 549-554, 1993.

[24] J. C. Behiri and W. Bonfield, "Fracture mechanics of bone- The effects of density, specimen thickness and crack velocity on longitudinal fracture", J Biomechanics, vol. 17(1), pp. 25-34, 1984.

[25] R. S. Lakes, S. Nakamura S., J. C. Behiri, W. Bonfield , "Fracture mechanics of bone with short cracks ", J Biomechanics, vol. 23(10), pp. 967-975, 1990.

[26] S. H. Advani, T. S. Lee, and R. B. Martin, "Analysis of crack arrest by cement lines in osteonal bone ", In 1987 Advances in bioengineering (Edited by Erdman, A. G.), ASME, New York, BED 3, pp. 57-88, 1987.

[27] R. M. V. Pidaparti and D. B. Burr, "Stress distribution on the Haversian canal due to microcracks in a cortical bone", ASME BED, vol. 20, pp. 357-359, 1991.

[28] J. N. Goodier, "Concentration of stress around spherical and cylindrical inclusions and flaws", Applied Mechanics, vol. 55, pp. 39-44, 1932.

[29] J. Dundurs and T. Mura, "Interaction between an edge dislocation and a circular inclusion", J Mech. phys. solids, vol. 12, pp. 177-189, 1964.

[30] D. M. Robertson., D. Robertson, and C. R. Barrett, "Fracture toughness, critical crack length and plastic zone size in bone", J Biomechanics, vol. 11, pp. 359-364, 1978.

[31] R. D. Crofts, T. M. Boyce, and C. Milgrom, "Aging changes in osteon mineralization in the human femoral neck", Bone, vol. 15, pp. 137-152, 1994.

[32] A. C. Courtney, W. C. Hayes, and L. J. Gibson, "Age-related differences in post-yield damage in human cortical bone. Experiment and model", J Biomechanics, vol. 29(11), pp. 1463-1471, 1996.

[33] T. M. Boyce, D. P. Fyhrie, M. C. Glotkowski, E. L. Radin, M. B. Schaffler, "Damage type and strain mode association in human compact bone bending fatigue ", J Orthopaedic Research, vol.16, pp. 322-329, 1998.